Appl. Math. Mech. -Engl. Ed., **42**(1), 127–142 (2021)

APPLIED MATHEMATICS AND MECHANICS (ENGLISH EDITION)

https://doi.org/10.1007/s10483-021-2677-9

Regular perturbation solution of Couette flow (non-Newtonian) between two parallel porous plates: a numerical analysis with irreversibility*

M. NAZEER[1], M. I. KHAN[2], S. KADRY[3], Yuming CHU[4,5,†], F. AHMAD[6], W. ALI[7], M. IRFAN[2], M. SHAHEEN[8]

1. Department of Mathematics, Institute of Arts and Sciences, Government College University, Chiniot Campus, Faisalabad 35400, Pakistan;
2. Department of Mathematics and Statistics, Riphah International University I-14, Islamabad 44000, Pakistan;
3. Department of Mathematics and Computer Science, Beirut Arab University, Beirut 11-5020, Lebanon;
4. Department of Mathematics, Huzhou University, Huzhou 313000, Zhejiang Province, China;
5. Hunan Provincial Key Laboratory of Mathematical Modeling and Analysis in Engineering, Changsha University of Science & Technology, Changsha 410114, China;
6. Department of Applied Sciences, National Textile University, Faisalabad 38000, Pakistan;
7. Chair of Production Technology, Faculty of Engineering Technology, University of Twente, Enschede 7500 AE, The Netherlands;
8. Department of Mathematics, Riphah Inernational Lniversity, Faisalabad Campus, Faiselabad 38000, Pakistan

(Received May 26, 2020 / Revised Aug. 6, 2020)

Abstract The unavailability of wasted energy due to the irreversibility in the process is called the entropy generation. An irreversible process is a process in which the entropy of the system is increased. The second law of thermodynamics is used to define whether the given system is reversible or irreversible. Here, our focus is how to reduce the entropy of the system and maximize the capability of the system. There are many methods for maximizing the capacity of heat transport. The constant pressure gradient or motion of the wall can be used to increase the heat transfer rate and minimize the entropy. The objective of this study is to analyze the heat and mass transfer of an Eyring-Powell fluid in a porous channel. For this, we choose two different fluid models, namely, the plane and generalized Couette flows. The flow is generated in the channel due to a pressure gradient or with the moving of the upper lid. The present analysis shows the effects of

* Citation: NAZEER, M., KHAN, M. I., KADRY, S., CHU, Y. M., AHMAD, F., ALI, W., IRFAN, M., and SHAHEEN, M. Regular perturbation solution of Couette flow (non-Newtonian) between two parallel porous plates: a numerical analysis with irreversibility. *Applied Mathematics and Mechanics* (*English Edition*), **42**(1), 127–142 (2021) https://doi.org/10.1007/s10483-021-2677-9

† Corresponding author, E-mail: chuyuming@zjhu.edu.cn

Project supported by the National Natural Science Foundation of China (Nos. 11971142, 11871202, 61673169, 11701176, 11626101, and 11601485)

the fluid parameters on the velocity, the temperature, the entropy generation, and the Bejan number. The nonlinear boundary value problem of the flow problem is solved with the help of the regular perturbation method. To validate the perturbation solution, a numerical solution is also obtained with the help of the built-in command NDSolve of MATHEMATICA 11.0. The velocity profile shows the shear thickening behavior via first-order Eyring-Powell parameters. It is also observed that the profile of the Bejan number has a decreasing trend against the Brinkman number. When $\eta_i \to 0\,(i = 1, 2, 3)$, the Eyring-Powell fluid is transformed into a Newtonian fluid.

Key words Couette flow, Eyring-Powell fluid, entropy generation, perturbation method, Bejan number

Chinese Library Classification O361
2010 Mathematics Subject Classification 76A05, 76A10, 76Rxx, 76Wxx

1 Introduction

The study in non-Newtonian fluids gets much attention of researchers due to its great importance in medical sciences, industries, and biological outcomes. It plays a vital role in bubble absorption, boiling, and polymer and plastic foam manufacturing. The relation between the stress and strain is more complex in non-Newtonian fluids as compared with that in Newtonian fluids. Further, these fluids deviate from Newton's law of viscosity. The nature of the non-Newtonian fluids cannot be understood from the single constitutive equation due to its complexity. Due to this fact, various non-Newtonian constitutive models have been presented by scientists and researchers such as the Sisko-fluid model, the Casson fluid model, the FENE-P fluid model, the Power-law fluid model, the viscoelastic fluid model, the micropolar fluid model, and the Eyring-Powell fluid model[1–10]. Ogunseye and Sibanda[11] worked on the Eyring-Powell fluid model subject to various boundary constraints. First, this fluid model is derived from the kinetic theory of fluids rather than the empirical relation. Second, this fluid model can be reduced into a Newtonian fluid in a certain shear rate. The model of an Eyring-Powell fluid can be used to formulate the flow of modern industrial materials such as ethylene glycol and powder graphite. The heat and mass transfer of an Eyring-Powell fluid in the channels and pipes has been studied by many researchers. Ali et al.[12] discussed the heat and mass transfer of an Eyring-Powell fluid in a pipe under the effect of viscous dissipation. They used the perturbation and shooting methods to handle the nonlinear boundary-value problems. The effect of variable viscosity on the Eyring-Powell fluid was analyzed by Nazeer et al.[13–14]. They used numerical and analytical techniques to solve the non-dimensional equations. The flow and heat transfer of an Eyring-Powell fluid in a porous channel was investigated by Khan et al.[15]. They used the homotopy analysis method and the shooting method based on Newton's Raphson method to obtain the solution to the problem. Riaz et al.[16] analyzed the effect of heat and mass transfer of an Eyring-Powell fluid within a rectangular complaint channel. They used the perturbation method to find the analytical expression of velocity and temperature fields. Waqas et al.[17] used the generalized Fourier's and Fick's laws to discuss the heat and mass transfer of an Eyring-Powell fluid over a stretching cylinder.

Recently, the major challenge in various industrial processes is the loss of energy. The attention of many researchers has been shifted towards the entropy generation in the flow of non-Newtonian fluids. The applications of entropy generation can be found in heat exchanger pumps and electronic cooling systems. Scientists and engineers are working to find methods on how to control the wastage of useful energy. For this, the second law of thermodynamics is the best, accurate, and eminent tool for optimizing a given system. According to Bejan[18], various investigations have been presented and available in the literature to minimize the entropy generation based on the second law of thermodynamics. For this, Sivaraj and Sheremet[19] analyzed the free convection flow with the effect of entropy generation of magnetohydrodynamic

(MHD) ferrofluids in a conduit which was heated from the bottom side. They used the finite difference scheme to solve the given nonlinear partial differential equations, and concluded that the mean heat transfer rate and mean entropy generation have the inverse relation via the magnetic parameter. The effect of the periodic magnetic field on the natural convection flow and entropy generation on a ferrofluid was investigated by Mehryan et al.[20]. The finite element method was used to solve the highly nonlinear boundary value problem. They observed that the mean heat transfer rate and the mean entropy generation of the uniform magnetic field are lower than the periodic magnetic field. Ganesh et al.[21] used the second-order thermal slip condition and entropy generation to investigate the buoyancy-driven flow of viscous fluid over a stretching surface.

Motivated by the above work, the research on entropy generation on the plane and generalized Couette flows of an Eyring-Powell fluid in a porous channel was carried out for the first time. We consider two flow phenomena, namely, the plane and generalized Couette flows, and calculate the velocity distribution, the temperature field, the entropy, and the Bejan numbers, separately with the help of the analytical and numerical approaches. For the analytical approach, we pick the perturbation method to solve both the systems. The built-in command of NDSolve in MATHEMATICA is chosen to validate the analytical solution. The computational results of both flow phenomena are discussed in a graphical form.

2 Mathematical formulations with geometry

Let us consider the two-type flows, namely, the plane and generalized Couette flows of the Eyring-Powell fluid in a horizontal porous channel, as shown in Fig. 1. The distance between the lower plate and the upper plate is $2H$, in which the lower and upper plates are set at $y = -H$, and $y = H$, respectively. It is assumed that the lower plate is maintained with the temperature θ_1, and the upper plate has a temperature θ_2. The dimensionless equations for the given flow problem with the boundary conditions are given as follows.

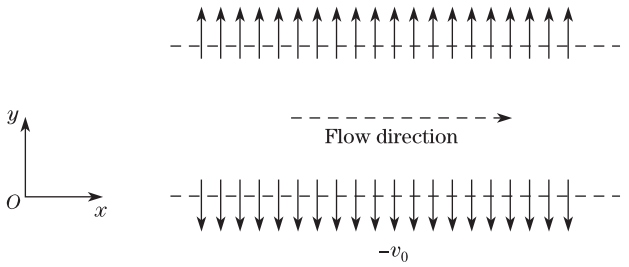

Fig. 1 Geometry of given problem

The component of the extra tensor of an Eyring-Powell fluid[22] is given by

$$\tau_{xy} = \overline{\mu}\frac{\partial u}{\partial y} + \frac{1}{\gamma}\arcsin\Big(\frac{1}{C}\frac{\partial u}{\partial y}\Big), \tag{1}$$

where $\overline{\mu}$ is called the dynamic velocity, and γ and C are known as the material fluid parameters. Use the Taylor's series expansion as

$$\arcsin\Big(\frac{1}{C}\frac{\partial u}{\partial y}\Big) = \frac{1}{C}\frac{\partial u}{\partial y} - \frac{1}{6}\Big(\frac{1}{C}\frac{\partial u}{\partial y}\Big)^3, \quad \Big|\frac{1}{C}\frac{\partial u}{\partial y}\Big| \ll 1. \tag{2}$$

The continuity equation is

$$\frac{\partial u}{\partial x} = 0. \tag{3}$$

The equation of motion is

$$\frac{\partial \tau_{xy}}{\partial y} + \rho v_0 \frac{\partial u}{\partial y} - \frac{\partial p}{\partial x} = 0. \tag{4}$$

The energy equation is

$$k\frac{\partial^2 \theta}{\partial y^2} + \tau_{xy}\frac{\partial u}{\partial y} + \rho C_P v_0 \frac{\partial \theta}{\partial y} = 0. \tag{5}$$

Substituting Eq. (2) into Eqs. (4)–(5), we obtain the new forms of Eqs. (4)–(5) as

$$\frac{\partial}{\partial y}\Big(\overline{\mu}\frac{\partial u}{\partial y} + \frac{1}{\gamma}\Big(\frac{1}{C}\frac{\partial u}{\partial y} - \frac{1}{6}\Big(\frac{1}{C}\frac{\partial u}{\partial y}\Big)^3\Big)\Big) + \rho v_0 \frac{\partial u}{\partial y} - \frac{\partial p}{\partial x} = 0, \tag{6}$$

$$k\frac{\partial^2 \theta}{\partial y^2} + \rho C_P v_0 \frac{\partial \theta}{\partial y} + \frac{\partial u}{\partial y}\Big(\overline{\mu}\frac{\partial u}{\partial y} + \frac{1}{\gamma}\Big(\frac{1}{C}\frac{\partial u}{\partial y} - \frac{1}{6}\Big(\frac{1}{C}\frac{\partial u}{\partial y}\Big)^3\Big)\Big) = 0, \tag{7}$$

where ρ, p, k, and C_P indicate the density, the pressure, the thermal conductivity, and the specific heat, respectively. The boundary conditions are given by

$$\begin{cases} u = 0, \quad \theta = \theta_1 \quad \text{at} \quad y = -H, \\ u = U_0, \quad \theta = \theta_2 \quad \text{at} \quad y = H, \end{cases} \tag{8}$$

where U_0, θ_1, and θ_2 are called the velocity of moving plate and the temperatures of the lower and upper walls of the channel, respectively.

To convert the above system of equations into a dimensionless form, we use the following dimensionless quantities:

$$\xi = \frac{y}{H}, \quad U = \frac{u}{U_0}, \quad T = \frac{\theta - \theta_1}{\theta_2 - \theta_1}. \tag{9}$$

With the help of the above equation, we obtain the dimensionless equations with the boundary conditions as

$$\frac{\mathrm{d}U}{\mathrm{d}x} = 0, \tag{10}$$

$$(1+\eta_1)\frac{\mathrm{d}^2 U}{\mathrm{d}\xi^2} + Re\frac{\mathrm{d}U}{\mathrm{d}\xi} - \eta_2 \frac{\mathrm{d}^2 U}{\mathrm{d}\xi^2}\Big(\frac{\mathrm{d}U}{\mathrm{d}\xi}\Big)^2 + P_x = 0, \tag{11}$$

$$\frac{\mathrm{d}^2\theta}{\mathrm{d}\xi^2} + Pe\frac{\mathrm{d}\theta}{\mathrm{d}\xi} + Br\Big((1+\eta_1)\Big(\frac{\mathrm{d}U}{\mathrm{d}\xi}\Big)^2 - \frac{\eta_3}{6}\Big(\frac{\mathrm{d}U}{\mathrm{d}\xi}\Big)^4\Big) = 0, \tag{12}$$

$$U(-1) = 0, \quad U(1) = 1, \quad T(-1) = 0, \quad T(1) = 1, \tag{13}$$

where

$$\eta_1 = \frac{1}{\overline{\mu}\gamma C}, \quad \eta_2 = \frac{\eta_1 v_0^2}{2H^2C^2}, \quad Pe = \frac{\overline{\rho} v_0 C_P}{k}, \quad Br = \frac{\overline{\mu} v_0^2}{k(\theta_2 - \theta_1)H^2}, \quad \eta_3 = \frac{v_0^2}{\overline{\mu}\gamma C^3 H^2}.$$

3 Plane Couette flow

In 1890, a French physicist Maurice Couette presented the concept of flow between two concentric cylinders to measure the viscosity of the fluids with the help of viscosimeter. This flow is commonly used to account the dynamic viscosity between the two-concentric cylinder and parallel plates. The plane Couette flow gives the simplest and easiest model to understand the phenomenon of heat and mass transfer between co-axial infinite (finite) cylinders or parallel channels. This type of flow is very important in lubrication, food processing, and polymer

solutions. The Couette flow is also known as a simple shear flow because it predicts the uniform shear stress distribution. In this flow, the velocity shows a linear relationship for the laminar flow's regime. In the plane Couette flow, both the boundaries (channel) have a different velocity. In our model, the fluid flows between two parallel porous plates due to the motion of the upper plate with the uniform velocity U_0 (moving along the x-axis direction), and the pressure gradient is zero. The equations of motion and energy for the present flow situation are given by

$$(1+\eta_1)\frac{\mathrm{d}^2U}{\mathrm{d}\xi^2}+Re\frac{\mathrm{d}U}{\mathrm{d}\xi}-\eta_2\frac{\mathrm{d}^2U}{\mathrm{d}\xi^2}\Big(\frac{\mathrm{d}U}{\mathrm{d}\xi}\Big)^2=0, \tag{14}$$

$$\frac{\mathrm{d}^2\theta}{\mathrm{d}\xi^2}+Pe\frac{\mathrm{d}\theta}{\mathrm{d}\xi}+Br\Big((1+\eta_1)\Big(\frac{\mathrm{d}U}{\mathrm{d}\xi}\Big)^2-\frac{\eta_3}{6}\Big(\frac{\mathrm{d}U}{\mathrm{d}\xi}\Big)^4\Big)=0, \tag{15}$$

$$U(-1)=0,\quad U(1)=1,\quad T(-1)=0,\quad T(1)=1. \tag{16}$$

Since an exact solution of the above developed system is not possible, to find the approximate analytical solution, we use the regular perturbation method taking ε as a perturbation parameter. For the continuous and convergent solution, we should have $0<\varepsilon\ll 1$[23]. The small values of the Brinkman number and the first-order non-dimensional Eyring-Powell parameter facilitate us to find the approximate analytical solution of the given problem. For this, we assume the velocity and temperature in the term of formal power series of ε^n $(n=0,1,2,\cdots)$.

$$U=U_0+\varepsilon U_1+O(\varepsilon^2),\quad T=T_0+\varepsilon T_1+O(\varepsilon^2),\quad \eta_2=\varepsilon\lambda,\quad Br=\varepsilon\delta. \tag{17}$$

Substituting Eq. (17) into Eqs. (14)–(16), we obtain the following zeroth- and first-order systems of ordinary equations with boundary conditions.

$O(\varepsilon^0)$:

$$(1+\eta_1)\frac{\mathrm{d}^2U_0}{\mathrm{d}\xi^2}+Re\frac{\mathrm{d}U_0}{\mathrm{d}\xi}=0, \tag{18}$$

$$\frac{\mathrm{d}^2T_0}{\mathrm{d}\xi^2}+Pe\frac{\mathrm{d}T_0}{\mathrm{d}\xi}=0, \tag{19}$$

$$U_0(-1)=0,\quad U_0(1)=1,\quad T_0(-1)=0,\quad T_0(1)=1. \tag{20}$$

$O(\varepsilon^1)$:

$$(1+\eta_1)\frac{\mathrm{d}^2U_1}{\mathrm{d}\xi_2}+Re\frac{\mathrm{d}U_1}{\mathrm{d}\xi}-\lambda\Big(\frac{\mathrm{d}U_0}{\mathrm{d}\xi}\Big)^2\Big(\frac{\mathrm{d}^2U_0}{\mathrm{d}\xi^2}\Big)=0, \tag{21}$$

$$\frac{\mathrm{d}^2T_1}{\mathrm{d}\xi^2}+Pe\frac{\mathrm{d}T_1}{\mathrm{d}\xi}+\delta\Big((1+\eta_1)\Big(\frac{\mathrm{d}U_0}{\mathrm{d}\xi}\Big)^2-\frac{\eta_3}{3}\Big(\frac{\mathrm{d}U_0}{\mathrm{d}\xi}\Big)^4\Big)=0, \tag{22}$$

$$U_1(-1)=U_1(1)=0,\quad T_1(-1)=T_1(1)=0. \tag{23}$$

Using the values of the constants of integration into Eq. (12) and some simplification, we obtain

$$U_0=\lambda_0+\lambda_1\mathrm{e}^{\frac{Re-Re\xi}{(1+\eta_1)}}. \tag{24}$$

To find the values of constants of integration, we have the imposed boundary conditions (23) and obtain

$$U_1=\lambda_2+\lambda_3\mathrm{e}^{-\frac{Re\xi}{(1+\eta_1)}}+\lambda_4\mathrm{e}^{-\frac{3Re(-1+\xi)}{(1+\eta_1)}}. \tag{25}$$

Combining the solution of the velocity profile, we obtain the final expression of the velocity profile in the original parameters as

$$U = \lambda_0 + \lambda_1 \mathrm{e}^{\frac{Re-Re\xi}{(1+\eta_1)}} + \lambda_2 + \lambda_3 \mathrm{e}^{-\frac{Re\xi}{(1+\eta_1)}} + \lambda_2 + \lambda_3 \mathrm{e}^{-\frac{Re\xi}{(1+\eta_1)}} + \lambda_4 \mathrm{e}^{-\frac{3Re(-1+\xi)}{(1+\eta_1)}}. \tag{26}$$

Putting the values of the constants of integration and making some simplification, we obtain

$$T_0 = \chi_0 + \chi_1 \mathrm{e}^{-Pe\xi}. \tag{27}$$

Solving the system of the temperature profile of order ε, we have

$$T_1 = \delta\big(\chi_2 + \chi_3 \mathrm{e}^{-Pe\xi} + \chi_4 \mathrm{e}^{-\frac{2Re(-1+\xi)}{(1+\eta_1)}} + \chi_5 \mathrm{e}^{-\frac{4Re(-1+\xi)}{(1+\eta_1)}}\big). \tag{28}$$

Combining the solution of the velocity profile, we obtain the final version of the temperature profile as follows:

$$T = \chi_0 + \chi_1 \mathrm{e}^{-Pe\xi} + Br\big(\chi_2 + \chi_3 \mathrm{e}^{-Pe\xi} + \chi_4 \mathrm{e}^{-\frac{2Re(-1+\xi)}{(1+\eta_1)}} + \chi_5 \mathrm{e}^{-\frac{4Re(-1+\xi)}{(1+\eta_1)}}\big). \tag{29}$$

3.1 Entropy generation and Bejan number of plane Couette flow

The normalized form of the total entropy number is given by

$$N_s = \Big(\frac{\mathrm{d}T}{\mathrm{d}\xi}\Big)^2 + \frac{Br}{\Omega}\Big((1+\eta_1) - \frac{\eta_3}{6}\Big(\frac{\mathrm{d}U}{\mathrm{d}\xi}\Big)^2\Big)\Big(\frac{\mathrm{d}U}{\mathrm{d}\xi}\Big)^2. \tag{30}$$

The first term in the above equation is due to heat generation and is denoted by N_{s_1}, while the second term comes due to viscous dissipation and is denoted by N_{s_2}, i.e.,

$$N_{s_1} = \Big(\frac{\mathrm{d}T}{\mathrm{d}\xi}\Big)^2, \quad N_{s_2} = \frac{Br}{\Omega}\Big((1+\eta_1) - \frac{\eta_3}{6}\Big(\frac{\mathrm{d}U}{\mathrm{d}\xi}\Big)^2\Big)\Big(\frac{\mathrm{d}U}{\mathrm{d}\xi}\Big)^2. \tag{31}$$

The analytical expressions of both terms are given by

$$\begin{aligned}
N_{s_1} &= \big(\mathrm{e}^{-Pe\xi}\chi_6 + \eta_3 Re\big(\mathrm{e}^{-\frac{Re\xi}{(1+\eta_1)}}\chi_7 + \mathrm{e}^{-\frac{2Re(-1+\xi)}{(1+\eta_1)}}\chi_8 + \mathrm{e}^{-\frac{4Re(-1+\xi)}{(1+\eta_1)}}\chi_9\big)\big)^2,\\
N_{s_2} &= \frac{Br}{\Omega}\big((1+\eta_1)\big(\mathrm{e}^{\frac{Re-Re\xi}{(1+\eta_1)}}\lambda_5 + \mathrm{e}^{-\frac{Re\xi}{(1+\eta_1)}}\lambda_6 + \mathrm{e}^{-\frac{3Re(-1+\xi)}{(1+\eta_1)}}\lambda_7\big)^2\\
&\quad - \frac{\eta_3}{6}\big(\mathrm{e}^{\frac{Re-Re\xi}{(1+\eta_1)}}\lambda_5 + \mathrm{e}^{-\frac{Re\xi}{(1+\eta_1)}}\lambda_6 + \mathrm{e}^{-\frac{3Re(-1+\xi)}{(1+\eta_1)}}\lambda_7\big)^4\big).
\end{aligned}$$

The total entropy number is defined by $N_s = N_{s_1} + N_{s_2}$.

The relation for the Bejan number is defined by

$$Be = \frac{N_{s_1}}{N_{s_1} + N_{s_2}}. \tag{32}$$

4 Generalized Couette flow

This physical model is similar to the previous flow model, i.e., the plane Couette flow. The difference between this model and the previous one is the pressure gradient. In the previous case, the fluid flows due to the motion of the upper plate, and the pressure gradient is zero. However, in this scenario, the pressure gradient is not zero. The upper plate is heated, and the lower one is cold, which is similar to the previous case. With the help of the perturbation technique, we obtain the system of each order as follows.

$O(\varepsilon^0)$:

$$(1+\eta_1)\frac{\mathrm{d}^2U_0}{\mathrm{d}\xi^2}+Re\frac{\mathrm{d}U_0}{\mathrm{d}\xi}+P_x=0, \tag{33}$$

$$\frac{\mathrm{d}^2T_0}{\mathrm{d}\xi^2}+Pe\frac{\mathrm{d}T_0}{\mathrm{d}\xi}=0, \tag{34}$$

$$U_0(-1)=0,\quad U_0(1)=1,\quad T_0(-1)=0,\quad T_0(1)=1. \tag{35}$$

$O(\varepsilon^1)$:

$$(1+\eta_1)\frac{\mathrm{d}^2U_1}{\mathrm{d}\xi^2}+Re\frac{\mathrm{d}U_1}{\mathrm{d}\xi}-\lambda\Big(\frac{\mathrm{d}U_0}{\mathrm{d}\xi}\Big)^2\Big(\frac{\mathrm{d}^2U_0}{\mathrm{d}\xi^2}\Big)=0, \tag{36}$$

$$\frac{\mathrm{d}^2T_1}{\mathrm{d}\xi^2}+Pe\frac{\mathrm{d}T_1}{\mathrm{d}\xi}+\delta\Big((1+\eta_1)\Big(\frac{\mathrm{d}U_0}{\mathrm{d}\xi}\Big)^2-\frac{\eta_3}{6}\Big(\frac{\mathrm{d}U_0}{\mathrm{d}\xi}\Big)^4\Big)=0, \tag{37}$$

$$U_1(-1)=U_1(1)=0,\quad T_1(-1)=T(1)=0. \tag{38}$$

Using the values of the constants of integration and making some simplification, we obtain

$$U_0=\lambda_8+\lambda_9\xi+\lambda_{10}\mathrm{e}^{-\frac{R\xi}{L}}. \tag{39}$$

To find the values of constants of integration, we impose the conditions and obtain

$$U_1=\lambda_{11}+\lambda_{12}\mathrm{e}^{-\frac{Re\xi}{(1+\eta_1)}}+\lambda_{13}\mathrm{e}^{-\frac{Re\xi}{(1+\eta_1)}}+\lambda_{14}\mathrm{e}^{-\frac{Re\xi}{(1+\eta_1)}}\xi+\lambda_{15}\mathrm{e}^{-\frac{2Re\xi}{(1+\eta_1)}}+\lambda_{16}\mathrm{e}^{-\frac{3Re\xi}{(1+\eta_1)}}. \tag{40}$$

Combining the solution of the velocity profile, we obtain the final version of the velocity profile as follows:

$$\begin{aligned}U=&\lambda_8+\lambda_9\xi+\lambda_{10}\mathrm{e}^{-\frac{Re\xi}{(1+\eta_1)}}+\lambda_{11}+\lambda_{12}\mathrm{e}^{-\frac{Re\xi}{(1+\eta_1)}}+\lambda_{13}\mathrm{e}^{-\frac{Re\xi}{(1+\eta_1)}}\\&+\lambda_{14}\mathrm{e}^{-\frac{Re\xi}{(1+\eta_1)}}\xi+\lambda_{15}\mathrm{e}^{-\frac{2Re\xi}{(1+\eta_1)}}+\lambda_{16}\mathrm{e}^{-\frac{3Re\xi}{(1+\eta_1)}}.\end{aligned} \tag{41}$$

By using the boundary conditions, we have the values of constants as follows:

$$T_0=\chi_{10}+\chi_{11}\mathrm{e}^{-Pe\xi}. \tag{42}$$

Solving the system of the temperature profile of order ε, we obtain

$$T_1=\delta\big(\chi_{12}+\chi_{13}\mathrm{e}^{-Pe\xi}+\chi_{14}\xi+\chi_{15}\mathrm{e}^{-\frac{Re\xi}{(1+\eta_1)}}+\chi_{16}\mathrm{e}^{-\frac{2Re\xi}{(1+\eta_1)}}+\chi_{17}\mathrm{e}^{-\frac{3Re\xi}{(1+\eta_1)}}+\chi_{18}\mathrm{e}^{-\frac{4Re\xi}{(1+\eta_1)}}\big). \tag{43}$$

Combining the solution of the velocity profile, we obtain the final version of the temperature profile as follows:

$$\begin{aligned}T=&\chi_{10}+\chi_{11}\mathrm{e}^{-Pe\xi}+Br\big(\chi_{12}+\chi_{13}\mathrm{e}^{-Pe\xi}+\chi_{14}\xi+\chi_{15}\mathrm{e}^{-\frac{Re\xi}{(1+\eta_1)}}\\&+\chi_{16}\mathrm{e}^{-\frac{2Re\xi}{(1+\eta_1)}}+\chi_{17}\mathrm{e}^{-\frac{3Re\xi}{(1+\eta_1)}}+\chi_{18}\mathrm{e}^{-\frac{4Re\xi}{(1+\eta_1)}}\big).\end{aligned} \tag{44}$$

4.1 Entropy generation and Bejan number of generalized Couette flow

The entropy numbers for the generalized Couette flow given by

$$\begin{aligned}N_{s_1}=&(\mathrm{e}^{-Pe\xi}\chi_{19}+Br(\chi_{14}+\mathrm{e}^{-Pe\xi}\chi_{20}+\mathrm{e}^{-\frac{Re\xi}{(1+\eta_1)}}\chi_{21}+\mathrm{e}^{-\frac{2Re\xi}{(1+\eta_1)}}\chi_{22}\\&+\mathrm{e}^{-\frac{3Re\xi}{(1+\eta_1)}}\chi_{23}+\mathrm{e}^{-\frac{4Re\xi}{(1+\eta_1)}}\chi_{24}))^2,\end{aligned} \tag{45}$$

$$\begin{aligned}N_{s_2}=&(1+\eta_1)(\lambda_9+\mathrm{e}^{-\frac{Re\xi}{(1+\eta_1)}}\lambda_{14}+\mathrm{e}^{-\frac{Re\xi}{(1+\eta_1)}}\lambda_{17}+\mathrm{e}^{-\frac{Re\xi}{(1+\eta_1)}}\lambda_{18}+\mathrm{e}^{-\frac{Re\xi}{(1+\eta_1)}}\lambda_{19}\\&+\mathrm{e}^{-\frac{Re\xi}{(1+\eta_1)}}\xi\lambda_{20}+\mathrm{e}^{-\frac{2Re\xi}{(1+\eta_1)}}\lambda_{21}+\mathrm{e}^{-\frac{3Re\xi}{(1+\eta_1)}}\lambda_{22})^2\\&-\frac{1}{6}\eta_3(\lambda_9+\mathrm{e}^{-\frac{Re\xi}{(1+\eta_1)}}\lambda_{14}+\mathrm{e}^{-\frac{Re\xi}{(1+\eta_1)}}\lambda_{17}+\mathrm{e}^{-\frac{Re\xi}{(1+\eta_1)}}\lambda_{18}+\mathrm{e}^{-\frac{Re\xi}{(1+\eta_1)}}\lambda_{19}\\&+\mathrm{e}^{-\frac{Re\xi}{(1+\eta_1)}}\xi\lambda_{20}+\mathrm{e}^{-\frac{2Re\xi}{(1+\eta_1)}}\lambda_{21}+\mathrm{e}^{-\frac{3Re\xi}{(1+\eta_1)}}\lambda_{22})^4.\end{aligned} \tag{46}$$

The relation for the Bejan number is defined by $Be = N_{s_1}/(N_{s_1} + N_{s_2})$.

5 Comparison with previous study

We compare our results with the results of Gupta and Massoudi[24] for the case of uniform viscosity model. Gupta and Massoudi[24] discussed the plane Couette flow of generalized second grade fluid between two heated walls for the case of Newtonian $m = 0$ and non-Newtonian $m \neq 0$ fluids under the consideration of constant and variable viscosity models. They set their plates at $y = 0$ and $y = H$, respectively. For comparison purpose, we set our channels at $y = 0$ and $y = H$. We present the values of velocity and temperature gradients for the Newtonian case against the variations of pressure gradient and viscous dissipation parameters in Table 1, and note that our solutions and those of Gupta and Massoudi[24] agree with each other.

Table 1 Comparison with Gupta and Massoudi[24], when $m = \eta_1 = \eta_2 = \eta_3 = Re = Pe = 0$

P_x	Br	Gupta and Massoudi[24]				Present			
		$U'(0)$	$U'(1)$	$T'(0)$	$T'(0)$	$U'(0)$	$U'(1)$	$T'(0)$	$T'(0)$
−2	0	0.999 0	−0.998 0	1.000 0	1.000 0	0.999 0	−0.998 0	1.000 0	1.000 0
−	2	0.999 0	−0.998 0	1.334 3	0.668 7	0.999 0	−0.998 0	1.334 3	0.668 7
−3	0	1.498 5	−1.497 0	1.000 0	1.000 0	1.498 5	−1.497 0	1.000 0	1.000 0
−	2	1.498 5	−1.497 0	1.749 3	0.254 5	1.498 5	−1.497 0	1.749 3	0.254 5

6 Results and discussion

The numerical, as well as perturbation solutions, are obtained for the flow of Eyring-Powell fluid in the porous channel. The upper and lower plates of the channel are set at the distance $2H$, in which the lower plate is set at $y = -H$ and the upper plates are at $y = 0$ and $y = H$. We discuss two main flow fields, namely, the plane Couette flow and the generalized Couette flow. The velocity distribution, the temperature field, the entropy generation, and the Bejan number are also discussed. The equations of motion and energy are solved and the analytical expressions of the velocity, the temperature, the entropy, and the Bejan number are found for both flow cases. We use the built-in command NDSolve in MATHEMATICA 11.0 for the validity of the perturbation solution. The ranges of the parameters are selected as follows.

The Eyring-Powell parameters $\eta_1 \in [0.1, 1]$, $\eta_2 \in [0.1, 1]$, $\eta_3 \in [0.1, 3]$, the Reynolds number $Re \in [1, 3]$, the Peclet number $Pe \in [1, 3]$, the Brinkman number $Br \in [0.1, 1]$, the Pressure gradient parameter $P_x \in [0.1, 2]$, and $\Omega = 0.017$. Figures 2 and 3 show the effects of various parameters on the velocity and temperature of the plane Couette flow. Figure 4 shows the effects of controlling parameters on the velocity and temperature of the generalized Couette flow. The total entropy number of the plane Couette flow is displayed via the length of the channel in Figs. 8 and 9, while the profiles of the Bejan number of the plane Couette flow are shown in Figs. 10 and 11. Similarly, the total entropy number and the Bejan number of the generalized Couette flow are presented in Figs. 12–15. The effects of the Eyring-Powell parameter η_1 and the Reynolds number on the velocity of the fluid are presented in Fig. 2. From this figure, it is observed that the velocity of the fluid has a decreasing behavior versus the Eyring-Powell parameter, while an opposite behavior is seen via the Reynolds number. It is noted that when $\eta_i \to 0\,(i = 1, 2, 3)$, the flow will be Newtonian, and the maximum velocity will be achieved in this situation. Further, the fluid gets thicker by increasing the values of the Eyring-Powell parameter η_i. As a result, the viscosity of the fluid decreases. Physically, the Eyring-Powell parameter predicts the shear-thickening effects. Figure 3 depicts the effects of the Peclet number and the Brinkman number. These figures show that the temperature of the fluid increases via the Peclet number and the Brinkman number in the entire length of the channel. Increasing the Brinkman number, the effect of viscous dissipation increases, and thus the temperature increases.

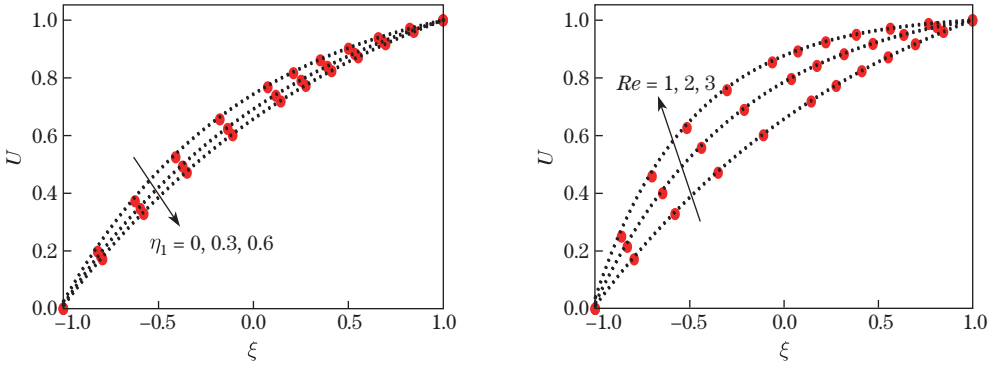

Fig. 2 Plots of velocity versus material parameter and Reynolds number (color online)

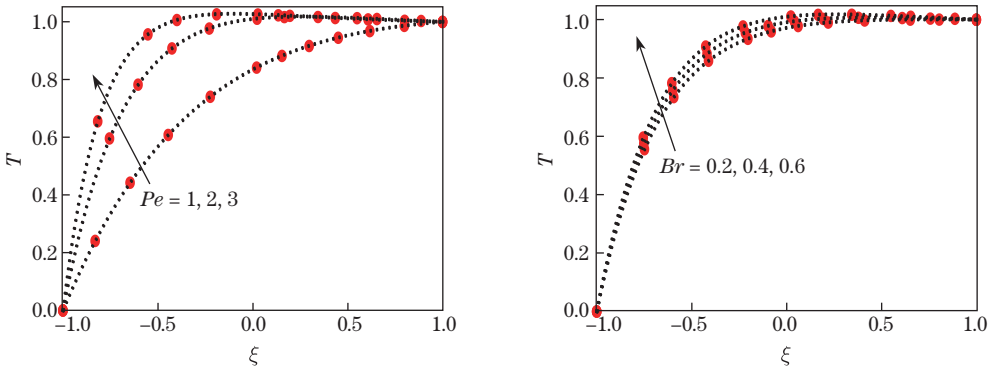

Fig. 3 Effects of Peclet and Brinkman numbers on temperature profile (color online)

The effects of the Eyring-Powell parameter, the Reynolds number, and the pressure parameter on the velocity of the generalized Couette flow are shown in Figs. 4 and 5. The same observation is made on the velocity via the Eyring-Powell parameter and the Reynolds number which we have explained in the previous case, i.e., the plane Couette flow. The new parameter, in this case, is the pressure gradient parameter which was missing in the previous case. The reason is that in the case of the plane Couette flow, the flow is just due to the top lid and the pressure gradient is not taken, for the case of generalized Couette flow, the source of the fluid flowing is a constant pressure gradient and motion of the top lid. The velocity of the generalized Couette flow increases with the increasing values of the pressure gradient parameter. The physical justification is that when more pressure is applied on the fluid, more fluid will take place in the plates with a higher velocity. Figures 6 and 7 depict the effects of the pressure gradient parameter, the Eyring-Powell parameter, the Brinkman number, and the Peclet number on the temperature profiles. It is noted that the temperature is an increasing function of the Brinkman number, the pressure gradient parameter, and the Peclet number, but a decreasing function of only the Eyring-Powell parameter. The effects of the Eyring-Powell parameters, the Brinkman number, and the Peclet number on the total entropy number are displayed in Figs. 8 and 9. The total entropy number shows an increasing trend via the Peclet number, the Eyring-Powell parameter, and the Brinkman number, and an opposite behavior is observed via the second Eyring-Powell parameter. It is observed that the total entropy number gets the maximum values at the left wall and approaches zero at the end of the channel. The profiles of the Bejan number versus the length of the channel under the effects of the Reynolds number, the Brinkman number, the Peclet number, and the first-order Eyring-Powell parameter are shown in Figs. 10 and 11. The profiles show that the Bejan number is the maximum at the end of the channel and the minimum at the start of the channel. It is also shown that the

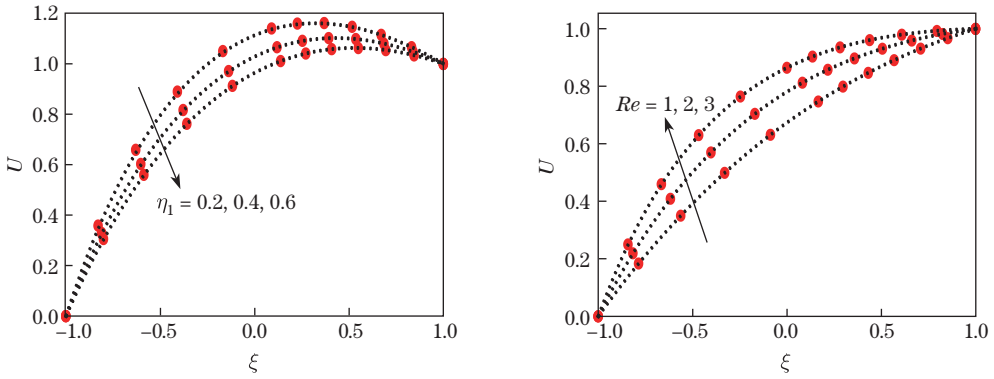

Fig. 4 Effects of material parameter and Reynolds number on velocity profile (color online)

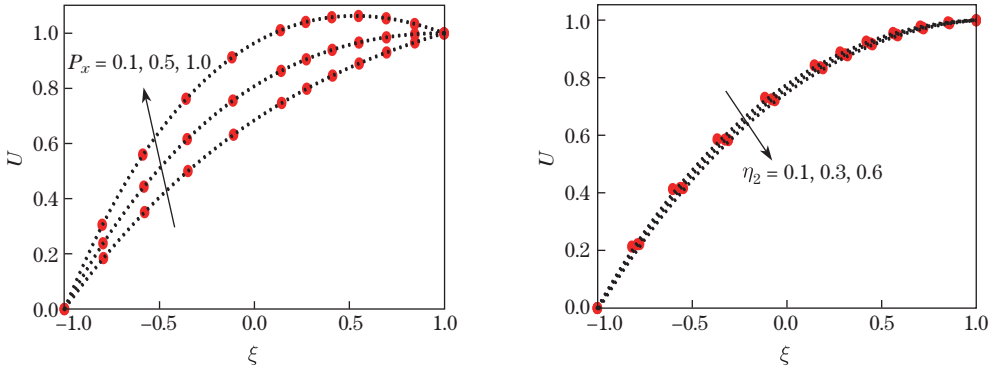

Fig. 5 Effects of pressure gradient parameter and material parameter on velocity profile (color online)

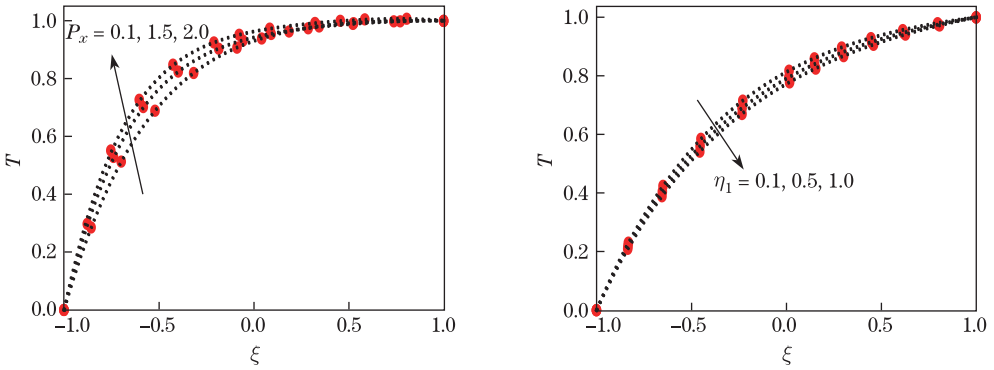

Fig. 6 Effects of pressure gradient parameter and material parameter on temperature profile (color online)

Bejan number decreases versus the Eyring-Powell parameter and increases via the Brinkman number and the Reynolds number in the whole interval $[-1, 1]$. On the other hand, the profile of the Bejan number shows an increasing trend in the interval of $[-1, 0]$ and a decreasing trend in $[0, 1]$, respectively, via the Peclet number. The profiles of the total entropy number and the Bejan number for the case of the generalized Couette flow are shown in Figs. 12–15. The same observation is captured on the total entropy number and the Bejan number versus the Eyring-Powell parameter, the Brinkman number, and the Reynolds number which we have already discussed in the previous case, i.e., the plane Couette flow. The entropy number has an increasing behavior versus the pressure gradient parameter in the interval $[-1, 0]$ and a

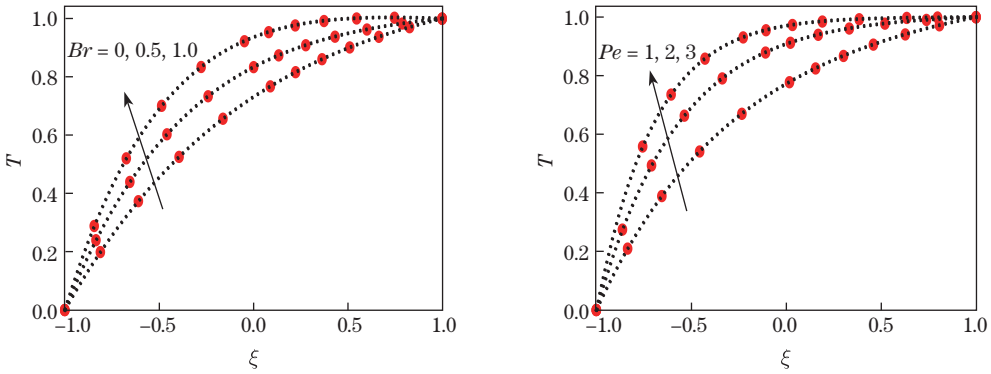

Fig. 7 Effects of Brinkman number and Peclet number on temperature profile (color online)

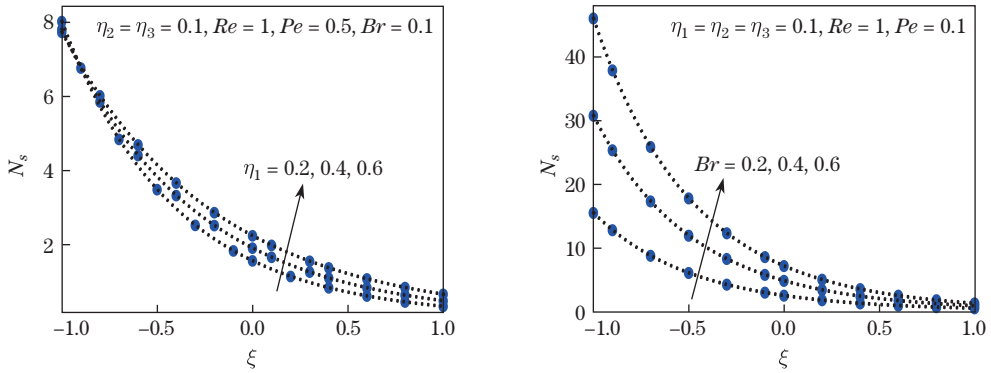

Fig. 8 Effects of material parameter and Brinkman number on entropy number (color online)

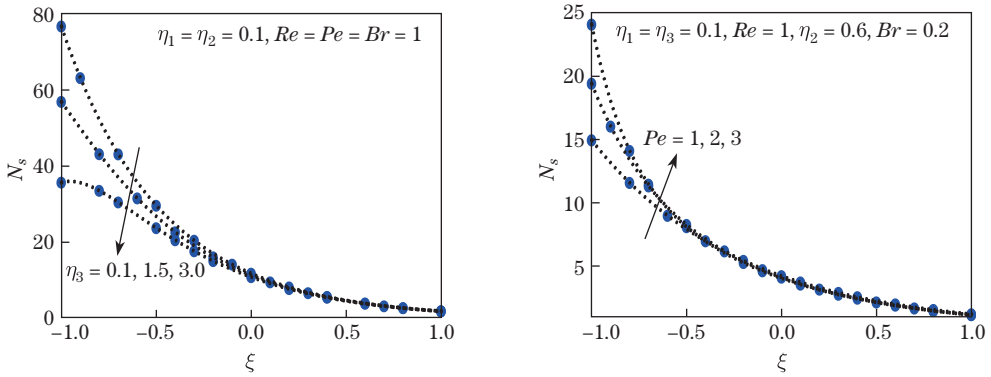

Fig. 9 Effects of material parameter and Peclet number on entropy number (color online)

decreasing trend in the rest of the channel. On the other hand, the Bejan number shows a decreasing trend in the interval $[-1, 0]$ and an increasing trend in $[0,\ 1]$ via the pressure gradient parameter.

7 Conclusions

The analytical and numerical solutions of the plane Couette flow and the generalized Couette flow of an Eyring-Powell fluid through a porous channel are investigated. In the present study,

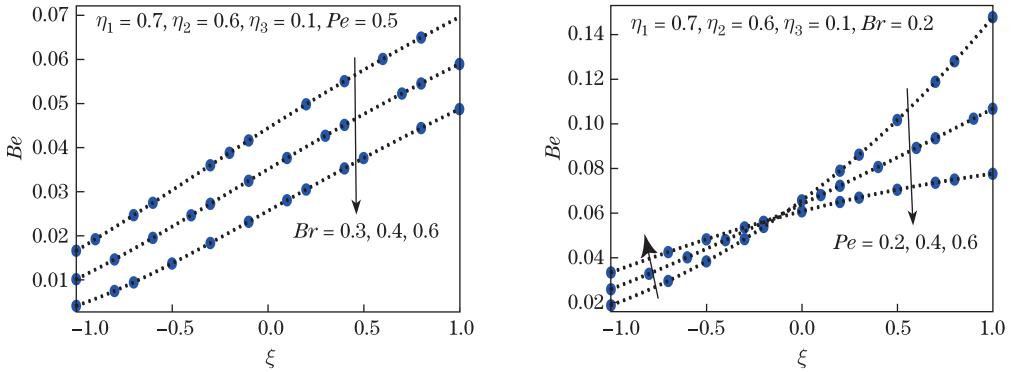

Fig. 10 Effects of Brinkman number and Peclet number on Bejan number (color online)

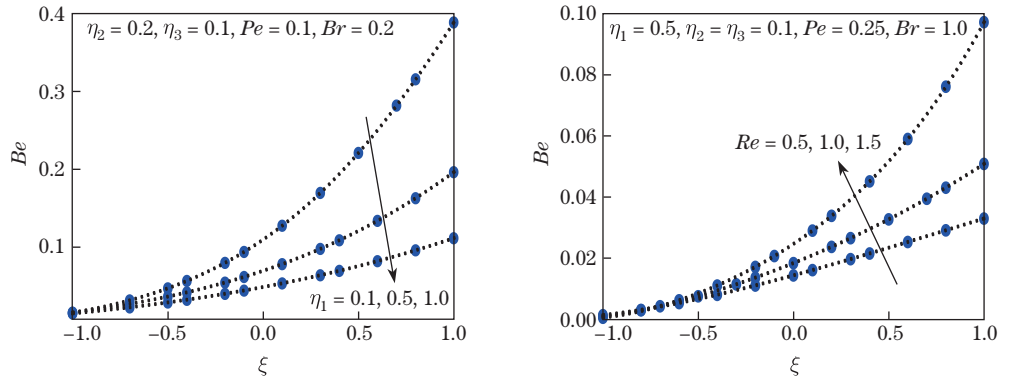

Fig. 11 Effects of material parameter and Reynolds number on Bejan number (color online)

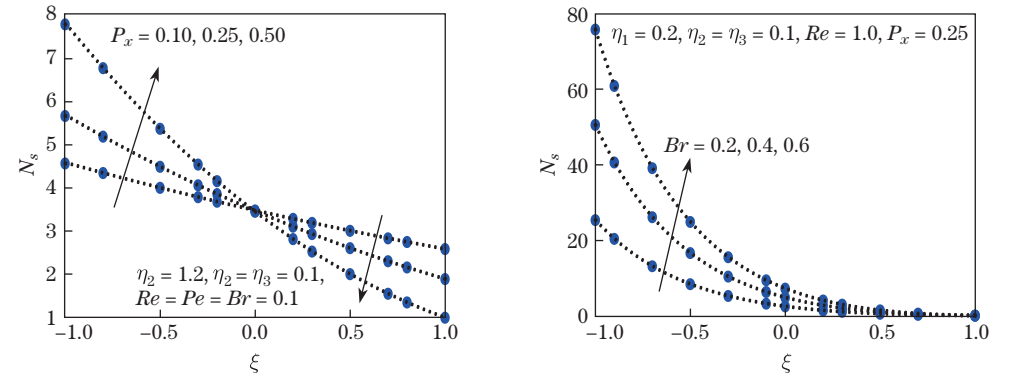

Fig. 12 Effects of pressure gradient parameter and Brinkman number on entropy number (color online)

we calculate the analytical solutions of the velocity and temperature profiles by using the perturbation technique. The numerical solution is also obtained by solving the direct dimensionless equation along with the boundary conditions with the help of the built-in command NDSolve of MATHEMATICA 11.0 software. From both solutions, it is noted that the perturbation solution is in good agreement with the numerical one. The effects of various physical parameters on the velocity, the temperature, the total entropy, and the Bejan numbers of both cases are captured with the help of the plots. The ranges of the physical parameter are also presented. The main findings of our study are summarized as follows.

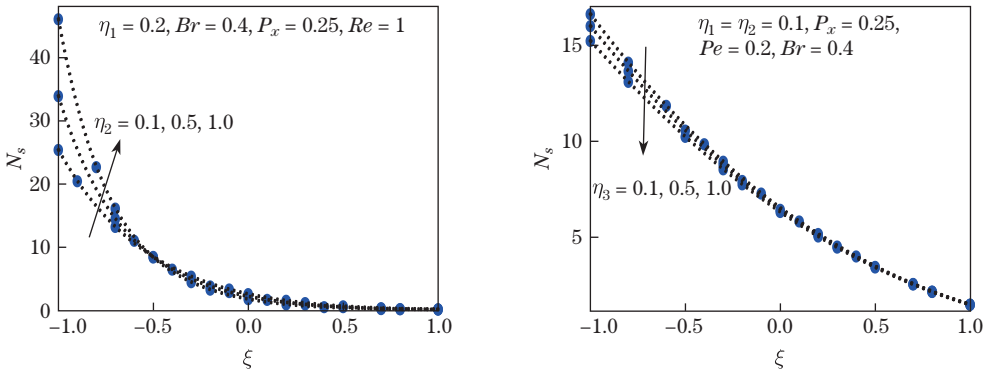

Fig. 13 Effects of material parameters on entropy number (color online)

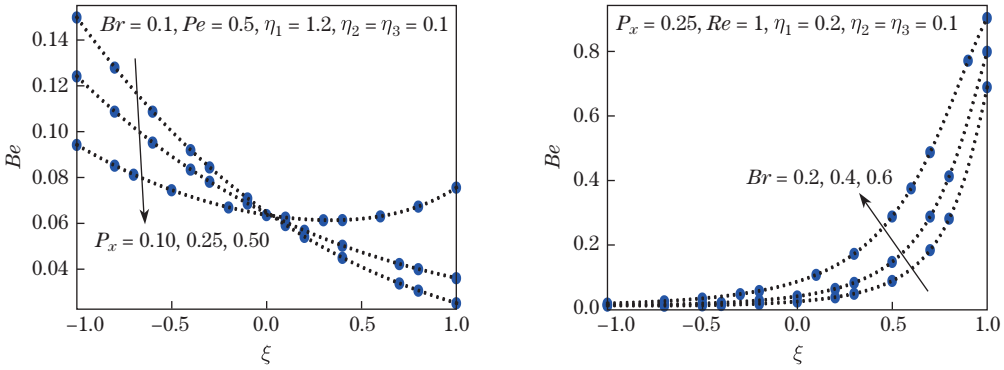

Fig. 14 Effects of pressure gradient parameter and Brinkman number on Bejan number (color online)

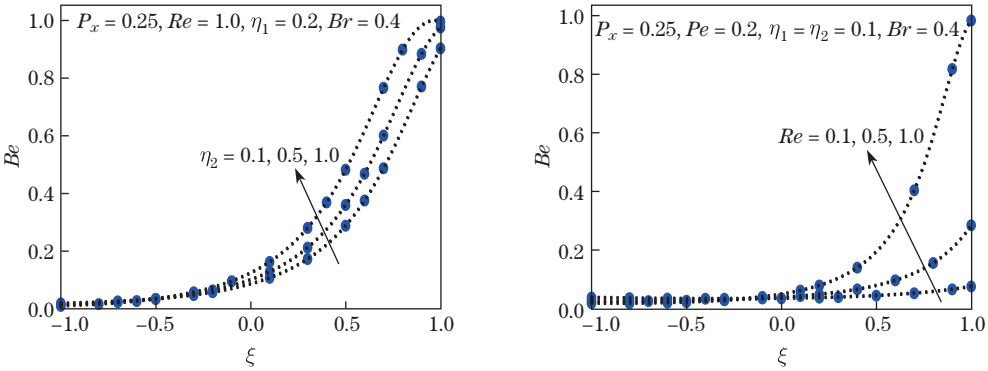

Fig. 15 Effects of material parameter and Reynolds number on Bejan number (color online)

(i) The first-order Eyring-Powell parameter predicts the shear-thickening behavior of the velocity.

(ii) When $\eta_i \to 0\,(i = 1, 2, 3)$, the Eyring-Powell fluid is transformed into a Newtonian fluid.

(iii) The velocity and the temperature of the fluid have an increasing behavior for all fluidic parameters except the first-order Eyring-Powell parameter.

(iv) The entropy generation is the maximum at the lower wall and approaches zero at the top wall.

(v) The entropy number increases near the lower wall via the first-order Eyring-Powell parameter, the Brinkman number, and the Peclet number, while the entropy number decreases via the third-order Eyring-Powell parameter.

(vi) The profile of the Bejan number decreases via the Brinkman number in the entire channel.

References

[1] KHAN, M. W. S. and ALI, N. Theoretical analysis of thermal entrance problem for blood flow: an extension of classical Graetz problem for Casson fluid model using generalized orthogonality relations. *International Communications in Heat and Mass Transfer*, **109**, 104314 (2019)

[2] KHAN, S. U., SHEHZAD, S. A., RAUF, A., and ALI, N. Mixed convection flow of couple stress nanofluid over oscillatory stretching sheet with heat absorption/generation effects. *Results in Physics*, **8**, 1223–1231 (2018)

[3] MUSTAFA, I., ABBAS, Z., ARIF, A., JAVED, T., and GHAFFARI, A. Stability analysis for multiple solutions of boundary layer flow towards a shrinking sheet: analytical solution by using least square method. *Physica A*: *Statistical Mechanics and Its Applications*, **540**, 123028(2020)

[4] FANG, T. G. and WANG, F. J. Momentum and heat transfer of a special case of the unsteady stagnation-point flow. *Applied Mathematics and Mechanics* (*English Edition*), **41**(1), 51–82 (2020) https://doi.org/10.1007/s10483-020-2556-9

[5] MAKINDE, O. D. Entropy-generation analysis for variable-viscosity channel flow with non-uniform wall temperature. *Applied Energy*, **85**, 384–393 (2008)

[6] NAG, P., MOLLA, M. M., and HOSSAIN, M. A. Non-Newtonian effect on natural convection flow over cylinder of elliptic cross section. *Applied Mathematics and Mechanics* (*English Edition*), **41**(2), 361–382 (2020) https://doi.org/10.1007/s10483-020-2562-8

[7] SUN, X., WANG, S., and ZHAO, M. Numerical solution of oscillatory flow of Maxwell fluid in a rectangular straight duct. *Applied Mathematics and Mechanics* (*English Edition*), **40**(11), 1647–1656 (2019) https://doi.org/10.1007/s10483-019-2535-6

[8] HAYAT, T. and ALI, N. On mechanism of peristaltic flows for power-law fluids. *Physica A*: *Statistical Mechanics and Its Applications*, **371**, 188–194 (2006)

[9] RAMESH, G. K., SHEHZAD, S. A., and TLILI, I. Hybrid nanomaterial flow and heat transport in a stretchable convergent/divergent channel: a Darcy-Forchheimer model. *Applied Mathematics and Mechanics* (*English Edition*), **41**(5), 699–710 (2020) https://doi.org/10.1007/s10483-020-2605-7

[10] ALSAEDI, A., HAYAT, T., QAYYUM, S., and YAQOOB, R. Eyring-Powell nanofluid flow with nonlinear mixed convection: entropy generation minimization. *Computer Methods and Programs in Biomedicine*, **186**, 105183 (2020)

[11] OGUNSEYE, H. A. and SIBANDA, P. A mathematical model for entropy generation in a Powell-Eyring nanofluid flow in a porous channel. *Heliyon*, **5**, e01662 (2019)

[12] ALI, N., NAZEER, F., and NAZEER, M. Flow and heat transfer analysis of Eyring-powell fluid in a pipe. *Zeitschrift für Naturforschung A*, **73**, 265–274 (2018)

[13] NAZEER, M., AHMAD, F., SALEEM, A., SAEED, M., NAVEED, S., SHAHEEN, M., and AIDAROUS, E. A. Effects of constant and space dependent viscosity on Eyring-Powell fluid in a pipe: comparison of perturbation and explicit finite difference method. *Zeitschrift für Naturforschung A*, **47**, 961–969 (2019)

[14] NAZEER, M., AHMAD, F., SAEED, M., SALEEM, A., KHALID, S., and AKRAM, Z. Numerical solution for flow of an Eyring-Powell fluid in a pipe with prescribed surface temperature. *Journal of the Brazilian Society of Mechanical Sciences and Engineering*, **41**, 518 (2019)

[15] KHAN, A. A., ZAIB, F., and ZAMAN, A. Effects of entropy generation on Powell Eyring fluid in a porous channel. *Journal of the Brazilian Society of Mechanical Sciences and Engineering*, **39**, 5027–5036 (2017)

[16] RIAZ, A., ELLAHI, R., BHATTI, M. M., and MARIN, M. Study of heat and mass transfer in the Eyring-Powell model of fluid propagating peristaltically through a rectangular compliant channel. *Heat Transfer Research*, **50**, 1539–1560 (2019)

[17] WAQAS, M., KHAN, M. I., HAYAT, T., ALSAEDI, A., and KHAN, M. I. On Cattaneo-Christov heat flux impact for temperature-dependent conductivity of Powell-Eyring liquid. *Chinese Journal of Physics*, **55**, 729–737 (2017)

[18] BEJAN, A. *Entropy Generation Minimization*, CRC, Boca Raton (1996)

[19] SIVARAJ, C. and SHEREMET, M. A. MHD natural convection and entropy generation of ferrofluids in a cavity with a non-uniformly heated horizontal plate. *International Journal of Mechanical Sciences*, **149**, 326–337 (2018)

[20] MEHRYAN, S. A. M., IZADI, M., CHAMKHA, A. J., and SHEREMET, M. A. Natural convection and entropy generation of a ferrofluid in a square enclosure under the effect of a horizontal periodic magnetic field. *Journal of Molecular Liquids*, **263**, 510–525 (2018)

[21] GANESH, N. V., MDALLAL, Q. M. A., and CHAMKHA, A. J. A numerical investigation of Newtonian fluid flow with buoyancy, thermal slip of order two and entropy generation. *Case Studies in Thermal Engineering*, **13**, 100376 (2019)

[22] AHMED, F., NAZEER, M., SAEED, M., SALEEM, A., and ALI, W. Heat and mass transfer of temperature-dependent viscosity models in a pipe: effects of thermal radiation and heat generation. *Zeitschrift für Naturforschung A*, **75**, 225–239 (2020)

[23] MURDOCK, J. Perturbation methods for engineers and scientists (Alan W. Bush). *SIAM Review*, **36**, 136–137 (1994)

[24] GUPTA, G. and MASSOUDI, M. Flow of a generalized second grade fluid between heated plates. *Acta Mechanica*, **99**, 21–33 (1993)

Appendix A

$$\lambda_0=\frac{1}{2}\Big(1+\coth\Big(\frac{Re}{(1+\eta_1)}\Big)\Big),\quad \lambda_1=-\frac{1}{2}\Big(-1+\coth\Big(\frac{Re}{(1+\eta_1)}\Big)\Big),$$

$$\lambda_2=\frac{\mathrm{e}^{\frac{2Re}{(1+\eta_1)}}\big(1+\mathrm{e}^{\frac{2Re}{(1+\eta_1)}}\big)Re^2\lambda_1^3}{6(1+\eta_1)^3},\quad \lambda_3=-\frac{\big(\mathrm{e}^{\frac{Re}{(1+\eta_1)}}+\mathrm{e}^{\frac{3Re}{(1+\eta_1)}}+\mathrm{e}^{\frac{5Re}{(1+\eta_1)}}\big)\lambda Re^2\lambda_1^3}{6(1+\eta_1)^3},$$

$$\lambda_4=\frac{\lambda Re^2\lambda_1^3}{6(1+\eta_1)^3},\quad \chi_0=\frac{1}{2}(1+\coth Pe),\quad \chi_1=-\frac{\operatorname{csch} Pe}{2},$$

$$\begin{aligned}\chi_2=&\,\delta Re(-1+\coth Pe)\lambda_1^2(-12\big(\mathrm{e}^{2Pe}-\mathrm{e}^{\frac{4Re}{(1+\eta_1)}}\big)(1+\eta_1)^3((1+\eta_1)Pe-4Re)\\&+\eta_3\big(\mathrm{e}^{2Pe}-\mathrm{e}^{\frac{8Re}{(1+\eta_1)}}\big)((1+\eta_1)Pe-2Re)Re^2\lambda_1^2)\\&\cdot(48(1+\eta_1)^2((1+\eta_1)Pe-4Re)((1+\eta_1)Pe-2Re)),\end{aligned}$$

$$\begin{aligned}\chi_3=&\,\delta\mathrm{e}^{Pe}\big(-1+\mathrm{e}^{\frac{4Re}{(1+\eta_1)}}\big)Re(-1+\coth Pe)\lambda_1^2(-12(1+\eta_1)^3((1+\eta_1)Pe-4Re)+\eta_3\big(1+\mathrm{e}^{\frac{4Re}{(1+\eta_1)}}\big)\\&\cdot((1+\eta_1)Pe-2Re)Re^2\lambda_1^2)(48(1+\eta_1)^2((1+\eta_1)Pe-4Re)((1+\eta_1)Pe-2Re)),\end{aligned}$$

$$\chi_4=\frac{\delta(1+\eta_1)Re\lambda_1^2}{2(1+\eta_1)Pe-4Re},\quad \chi_5=-\frac{\eta_3\delta Re^3\lambda_1^4}{24(1+\eta_1)^2((1+\eta_1)Pe-4Re)},\quad \chi_6=Pe\chi_1,\quad \chi_7=-Pe\chi_3,$$

$$\chi_8=-\frac{2Re\chi_4}{(1+\eta_1)},\quad \chi_9=-\frac{4Re\chi_5}{(1+\eta_1)},\quad \lambda_5=-\frac{Re\lambda_1}{(1+\eta_1)},\quad \lambda_6=-\frac{2Re\lambda_3}{(1+\eta_1)},\quad \lambda_7=-\frac{3Re\lambda_4}{(1+\eta_1)},$$

$$\lambda_8=\frac{Re+(2P_x+Re)\coth\frac{Re}{(1+\eta_1)}}{2Re},\quad \lambda_9=\frac{-P_x}{Re},\quad \lambda_{10}=-\frac{(2P_x+Re)\operatorname{csch}\frac{Re}{(1+\eta_1)}}{2Re},$$

$$\lambda_{11}=\lambda Re\lambda_2\Big(3(1+\eta_1)\operatorname{csch}\frac{Re}{(1+\eta_1)}\lambda_1^2-3(1+\eta_1)\lambda_1\lambda_2+Re\cosh\frac{Re}{(1+\eta_1)}\lambda_2^2\Big)3(1+\eta_1)^3,$$

$$\lambda_{12} = \lambda\lambda_2(6(1+\eta_1)\Big((1+\eta_1) - Re\coth\frac{Re}{(1+\eta_1)}\Big)\lambda_1^2 + 12(1+\eta_1)Re\operatorname{cosh}\frac{Re}{(1+\eta_1)}\lambda_1\lambda_2$$
$$- Re^2\Big(1 + 2\operatorname{cosh}\frac{2Re}{(1+\eta_1)}\Big)\lambda_2^2)6(1+\eta_1)^3,$$
$$\lambda_{13} = -\frac{\lambda\lambda_1^2\lambda_2}{(1+\eta_1)}, \quad \lambda_{14} = -\frac{\lambda Re\lambda_1^2\lambda_2}{(1+\eta_1)^2}, \quad \lambda_{15} = -\frac{\lambda Re\lambda_1\lambda_2^2}{(1+\eta_1)^2}, \quad \lambda_{16} = \frac{\lambda Re^2\lambda_2^3}{6(1+\eta_1)^3},$$
$$M_6 = -(72(1+\eta_1)^2Pe((1+\eta_1)Pe-4Re)((1+\eta_1)Pe-3Re)((1+\eta_1)Pe-2Re)((1+\eta_1)Pe-Re))^{-1},$$
$$\chi_{10} = \frac{1}{2}(1+\coth Pe), \quad \chi_{11} = -\frac{\operatorname{csch} Pe}{2}, \quad \chi_{10} = \frac{1}{2}(1+\coth Pe), \quad \chi_{11} = -\frac{\operatorname{csch} Pe}{2}, \quad \chi_{12} = M_6M_7,$$
$$\chi_{13} = \frac{\mathrm{e}^{Pe}(-1+\coth Pe)}{72}\Big(\frac{12\lambda_1^2\left(-6(1+\eta_1)+\eta_3\lambda_1^2\right)}{Pe} + \frac{48(1+\eta_1)\sinh\frac{Re}{(1+\eta_1)}\lambda_1\left(3(1+\eta_1)-\eta_3\lambda_1^2\right)\lambda_2}{(1+\eta_1)Pe-Re}$$
$$- \frac{36Re\sinh\frac{2Re}{(1+\eta_1)}\left((1+\eta_1)-\eta_3\lambda_1^2\right)\lambda_2^2}{(1+\eta_1)Pe-2Re} - \frac{16\eta_3Re^2\sinh\frac{3Re}{(1+\eta_1)}\lambda_1\lambda_2^3}{(1+\eta_1)^2Pe-3(1+\eta_1)Re}$$
$$+ \frac{3\eta_3Re^3\sinh\frac{4Re}{(1+\eta_1)}\lambda_2^4}{(1+\eta_1)^2((1+\eta_1)Pe-4Re)}\Big),$$
$$\chi_{19} = -Pe\chi_{11}, \quad \chi_{20} = -Pe\chi_{13}, \quad \chi_{21} = -\frac{Re\chi_{15}}{(1+\eta_1)}, \quad \chi_{22} = -\frac{2Re\chi_{16}}{(1+\eta_1)},$$
$$\chi_{23} = -\frac{3Re\chi_{17}}{(1+\eta_1)}, \quad \chi_{24} = -\frac{4Re\chi_{18}}{(1+\eta_1)}, \quad \lambda_{17} = -\frac{Re\lambda_{10}}{(1+\eta_1)}, \quad \lambda_{18} = -\frac{Re\lambda_{12}}{(1+\eta_1)},$$
$$\lambda_{19} = -\frac{Re\lambda_{13}}{(1+\eta_1)}, \quad \lambda_{20} = -\frac{Re\lambda_{14}}{(1+\eta_1)}, \quad \lambda_{21} = -\frac{2Re\lambda_{15}}{(1+\eta_1)}, \quad \lambda_{22} = -\frac{3Re\lambda_{16}}{(1+\eta_1)},$$
$$M_7 = \mathrm{e}^{-\frac{Re}{(1+\eta_1)}}(-1+\coth Pe)(6\eta_3\mathrm{e}^{\frac{Re}{(1+\eta_1)}}(1+\mathrm{e}^{2Pe})(1+\eta_1)^2((1+\eta_1)Pe-4Re)$$
$$\cdot((1+\eta_1)Pe-3Re)((1+\eta_1)Pe-2Re)((1+\eta_1)Pe-Re)\lambda_1^4 + 24\eta_3\left(\mathrm{e}^{2Pe} - \mathrm{e}^{\frac{2Re}{(1+\eta_1)}}\right)$$
$$\cdot(1+\eta_1)^3Pe((1+\eta_1)Pe-4Re)((1+\eta_1)Pe-3Re)((1+\eta_1)Pe-2Re)\lambda_1^3\lambda_2)$$
$$- 3\mathrm{e}^{Pe+\frac{Re}{(1+\eta_1)}}(Pe((1+\eta_1)Pe-3Re)((1+\eta_1)Pe-Re)Re\lambda_2^2)$$
$$\cdot\Big(-12(1+\eta_1)^3((1+\eta_1)Pe-4Re)\sinh\Big(Pe-\frac{2Re}{(1+\eta_1)}\Big)$$
$$+ \eta_3((1+\eta_1)Pe-2Re)Re^2\sinh\Big(Pe-\frac{4Re}{(1+\eta_1)}\Big)\lambda_2^2\Big)$$
$$- 16\mathrm{e}^{Pe+\frac{Re}{(1+\eta_1)}}(1+\eta_1)Pe((1+\eta_1)Pe-4Re)((1+\eta_1)Pe-2Re)$$
$$\cdot\lambda_1\lambda_2\Big(9(1+\eta_1)^3((1+\eta_1)Pe-3Re)\sinh\Big(Pe-\frac{Re}{(1+\eta_1)}\Big)$$
$$+ \eta_3Re^2(-(1+\eta_1)Pe+Re)\sinh\Big(Pe-\frac{3Re}{(1+\eta_1)}\Big)\lambda_2^2\Big)$$
$$- 36\mathrm{e}^{Pe+\frac{Re}{(1+\eta_1)}}(1+\eta_1)^2((1+\eta_1)Pe-4Re)$$
$$\cdot((1+\eta_1)Pe-3Re)((1+\eta_1)Pe-Re)\lambda_1^2$$
$$\cdot\Big(2(1+\eta_1)((1+\eta_1)Pe-2Re)\cosh Pe + \eta_3PeRe\sinh\Big(Pe-\frac{2Re}{(1+\eta_1)}\Big)\lambda_2^2\Big),$$
$$\chi_{14} = \frac{\lambda_1^2\left(-6(1+\eta_1)+\eta_3\lambda_1^2\right)}{6Pe}, \quad \chi_{15} = \frac{2(1+\eta_1)\lambda_1\left(-3(1+\eta_1)+\eta_3\lambda_1^2\right)\lambda_2}{3(1+\eta_1)Pe-3Re},$$
$$\chi_{16} = \frac{Re\left((1+\eta_1)-\eta_3\lambda_1^2\right)\lambda_2^2}{2(1+\eta_1)Pe-4Re}, \quad \chi_{17} = \frac{2\eta_3Re^2\lambda_1\lambda_2^3}{9(1+\eta_1)^2Pe-27(1+\eta_1)Re},$$
$$\chi_{18} = -\frac{\eta_3Re^3\lambda_2^4}{24(1+\eta_1)^2((1+\eta_1)Pe-4Re)}.$$